MITT.ÖSTERR.MINER.GES. 153 (2007)

MUSCOVITE-CHLORITE-QUARTZ THERMOBAROMETRY OF THE PERMIAN METAMORPHIC OVERPRINT OF THE CENTRAL PART OF THE WESTERN INNSBRUCK QUARTZPHYLLITE COMPLEX (TYROL, AUSTRIA)

by

Andreas Piber & Peter Tropper

Institute of Mineralogy and Petrography
Faculty of Geo- and Atmospheric Sciences
Leopold-franzens University of Innsbruck, Innrain 52, A-6020 Innsbruck, Austria

Abstract

The Innsbruck Quartzphyllite Complex (IQP) is part of the Austroalpine basement nappes north of the Tauern Window. In the central part of the western IQP garnet-mica-schists with the mineral assemblage garnet + muscovite + chlorite + garnet + plagioclase occur. Microstructural evidence indicates that the equilibrium assemblage is muscovite + chlorite + quartz, which allows application of the method of VIDAL & PARRA (2000) by considering all possible equilibria among the phase components (muscovite, celadonite, pyrophyllite, clinochlore, Mg-amesite) of this assemblage. Although not unproblematic due to consideration of phase components in muscovite solid solutions involving the vacancy on the A-site, muscovite-chlorite-quartz thermobarometry yielded 500 ± 50°C and 4.5 ± 2 kbar for the garnet mica schists of the central part of the western IQP. Geochronological data from metaporphyroids and quartzphyllites from this area indicate that these P-T conditions most likely represent the Permian event in the western IQP.

Geological Overview

The polymetamorphic crystalline basement north of the Tauern Window is comprised of lower Ordovician porphyroid-gneisses (Kellerjochgneiss/Schwazer Augengneiss), micaschists and gneisses (Patscherkofel and Glungezer Crystalline Complex) and Paleozoic schists (Innsbruck Quartzphyllite Complex and Wildschönau Schists) with intercalated carbonates (Schwaz Dolomite) (Fig. 1).

First intensive mapping investigations of the crystalline basement nappes north of the Tauern Window were performed at the beginning of the 20th century by AMPFERER & OHNESORGE (1918, 1924). Further extended field investigations of the IQP were done in the second part of the 20th century by SCHMIDEGG (1964), GWINNER (1971), SATIR & MORTEANI (1978a, b), HOSCHEK et al. (1980), SATIR et al. (1980), MOSTLER et al. (1982), HADITSCH & MOSTLER (1982, 1983) and ROTH (1983).

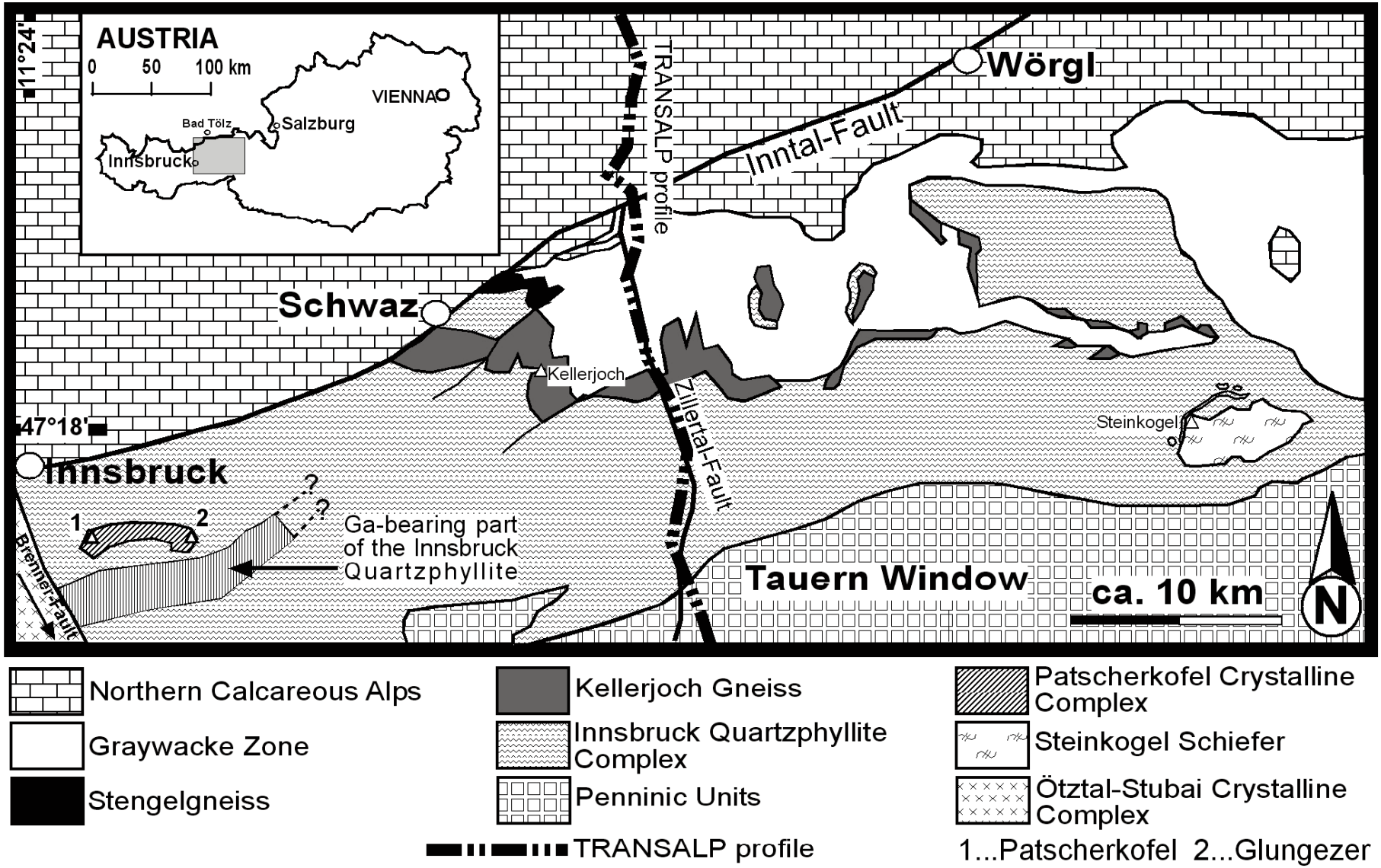

Fig. 1

Geographical and Geological overview of the area of investigation, which is located in the central part of Tyrol. Note the TRANSALP profile in the center of the image crosscutting all tectonic units.

Due to its monotonous appearance, the IQP was considered an undifferentiated mass for a long period. HADITSCH & MOSTLER (1982, 1983) were the first to introduce a serial differentiation on the base of intercalated lithologies within the quartzphyllites. The most recent studies of KOLENPRAT et al. (1999) and ROCKENSCHAUB et al. (2003) confirm and complete HADITSCH & MOSTLER (1982, 1983) serial differentiation. In addition, in the last years, Permian and Eo-Alpine mica cooling ages from the quartzphyllites and Permian ages of intercalated metaporphyroids in the quartzphyllite basement became available (ROCKENSCHAUB et al., 2003). Zircons, derived from metaporphyroids, yielded U/Pb ages, which were attributed to a temperature-accentuated Permian event. These ages were also confirmed by Rb/Sr cooling ages of white micas of the same lithologies (ROCKENSCHAUB et al., 2003). Since the central part of the western IQP is the only part of the IQP that shows no evidence for an Eo-Alpine rejuvination so far, this part represents the ideal study area for deducing the Permian P-T conditions.

Lithologies of the central western IQP

The quartzphyllites, occur as low-grade metamorphic pelites and psammites with variable amounts of quartz and feldspar. Sericite phyllites, chlorite phyllites and mica-bearing quartzites occur subordinated. Diameters of mostly lens shaped quartz intercalations within the quartzphyllites vary from a few cm up to several dm. The mineral assemblage of the quartzphyllites is represented by muscovite + chlorite + albite-rich feldspar + quartz ± biotite. Accessory minerals are calcite, rutile, ilmenite, tourmaline, zircon and graphite.

To the south of the tectonic contact between the IQP and the Patscherkofel Crystalline Complex, garnet-micaschists occur. The northern border of this garnet-micaschist is about 200 meters to the south of the Glungezer and the micaschists extent to the region of the Kreuzspitze in the South. The total diameter of the garnet micaschists is about 1400 m. These schists are crosscut by orthogneiss dikes of several tens of meters in the region around the Gamslahner. Also several intercalations of thin layers of porphyroid-gneisses, greenschists and metacarbonates occur and thus can be used as stratigraphic marker lithologies. The garnet-micaschists do not occur North of the Patscherkofel Crystalline Complex, but were also confirmed in the course of a drilling project during a prospection campaign in the region around the Village of Igls (ROCKENSCHAUB et al., 2003). In the East, the diameter of the garnet-micaschists decreases and towards the eastern regions it totally disappears, which might be caused by tectonical thinning. The mineral assemblage of the garnet-micaschist is represented by garnet + muscovite + chlorite + albite-rich plagioclase + quartz. The accessories are ilmenite, rutile and clinozoisite. The absence of biotite in these schists is remarkable. Garnets occur as porphyroblasts with diameters of up to 1 cm. The amount of garnets within the micaschist varies locally. The diameter of the garnets increases from North to South. As an expression of the subsequent retrograde overprint garnet rims are replaced by chlorite and thus garnet is not considered to be in equilibrium with the surrounding mineral assemblage and was not used for thermobarometric calculations.

Mineral chemistry

Mineral compositions were measured with the JEOL SUPERPROBE X-8100 electron microprobe at the Institute of Mineralogy and Petrography of the University of Innsbruck. Operation conditions were 15 kV at a sample current of 20 nA, except sheet silicates which were measured

with a reduced sample current of 10 nA and a rastered beam with a raster size between 2 and 5 μm to prevent loss of alkalies. Natural and synthetical standards were used for calibration. Mineral formulae calculations were performed with the programs MacAX (HOLLAND, 1999; written comm.), Norm II (ULMER, 1999; written comm.) and Hyperform96 (BJERG et al., 1992).

Garnet: Garnets mostly occur as porphyroblasts with diameters ranging up to 5 mm. The garnets show no mineral inclusions indicating a penetrative foliation. All garnets are almandine rich (Alm $_{47\text{-}83}$) with smaller amounts of pyrope- ($Prp_{2\text{-}12}$), grossular- ($Grs_{6\text{-}34}$) and spessartine- ($Sps_{0.5\text{-}16}$) components (Tab. 1). X-ray distribution images show a decrease of iron and magnesium during continuous mineral growth. In the southernmost part of the garnet-micaschist, garnets with larger diameters occur. The prograde chemical zoning is based on bell-shaped element distributions with decreasing amounts of X_{Alm} and X_{Prp} and increasing X_{Sps} from rim to core. (Fig. 2).

Sample	IQP-P6b	IQP-P6b	IQP-P6b	IQP-P19	IQP-P19	IQP-P19
	ga1	ga5	ga12	Ga57	Ga67	Ga111
SiO_2	37.25	36.95	36.97	37.42	37.38	37.60
TiO_2	n.d.	0.03	n.d.	0.15	0.09	0.04
Al_2O_3	20.92	21.04	21.16	20.73	20.51	20.73
Cr_2O_3	n.c.	0.19	0.02	n.d.	0.02	n.d.
Fe_2O_3	1.57	1.07	0.91	n.c.	n.c.	n.c.
FeO	32.62	32.70	34.01	30.24	30.56	32.94
MnO	1.21	1.34	1.19	6.06	6.09	2.92
MgO	1.64	1.43	1.37	0.85	0.91	1.25
CaO	5.43	5.61	4.75	5.04	4.92	4.52
Na_2O	0.11	0.09	0.02	0.02	0.02	n.d.
K_2O	0.10	n.d.	0.12	0.01	0.01	n.d.
Total	100.85	100.45	100.52	100.52	100.51	100.00
Si	2.980	2.970	2.976	3.017	3.019	3.035
Ti	n.d.	0.002	n.d.	0.009	0.005	0.002
Al	1.973	1.994	2.008	1.970	1.953	1.973
Cr	n.d.	0.012	0.001	n.d.	n.d.	0.001
Fe^{3+}	0.094	0.065	0.055	n.c.	n.c.	n.c.
Fe^{2+}	2.182	2.198	2.290	2.039	2.064	2.224
Mn	0.082	0.091	0.081	0.414	0.417	0.200
Mg	0.196	0.171	0.164	0.102	0.110	0.150
Ca	0.465	0.483	0.410	0.435	0.426	0.391
Na	0.017	0.014	0.003	0.003	0.003	n.d.
K	0.010	n.d.	0.012	0.001	0.001	n.d.
Sum	8.000	8.000	8.000	7.991	8.000	7.976

Calculations on the base of 12 oxygens, n.d.: not detected; n.c.:not calculated

Table 1

Representative garnet analyses

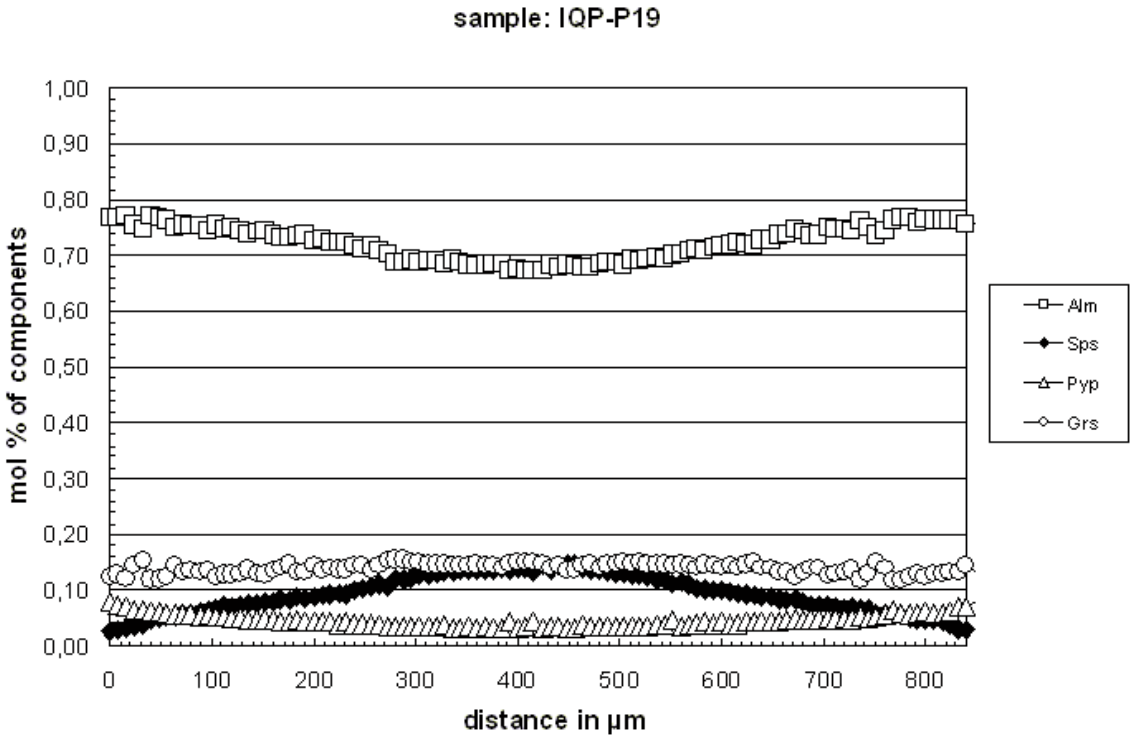

Fig. 2

Plot illustrating the continuous chemical zonation of garnet of a garnet-micaschist of the central part of the western IQP (sample IQP-P19).

Muscovite: Chemically, the white micas are homogeneous. The Si contents vary from 3.07 to 3.29 a.p.f.u. (Tab. 2). The paragonite component varies between 4.8 and 10.9 mol.%. The margarite component of all muscovites is below 2 mol.%.

Chlorite: Chlorites are closely intergrown with muscovite (Fig. 3). The Fe contents vary between 2.18 and 2.71 a.p.f.u. and Mg contents lie between 1.69 and 2.38 a.p.f.u. The Fe/Fe+Mg ratio ranges from 0.48 to 0.61 (Tab. 3) and Al_{tot} contents range from 2.65 to 2.96 a.p.f.u.. According to the chemical classification of HEY (1954) the chlorites are rhipidolites.

Feldspars: In the central parts of the western quartzphyllites feldspars show anorthite-bearing cores (An_{6-12} Ab_{85-93} Or_{1-4}) and nearly pure albite rims (An_{1-2} Ab_{98-99} Or_{0-2}).

Thermobarometry

Thermobarometry according to the method of VIDAL & PARRA (2000) of the biotite-absent garnet mica schist samples of the central western IQP was performed with the program TWQ v.2.02b (BERMAN, 1988, 1992 written comm.) with the dataset of VIDAL (2002, written comm.) in the system K_2O-MgO-Al_2O_3-SiO_2-H_2O (KMASH). This method allows calculation of all possible reactions between the end-members of chlorite (Mg-amesite, clinochlore) and muscovite (muscovite, celadonite, pyrophyllite) with quartz and H_2O in excess. Although internal consistency with the database of BERMAN (1988, 1992, written comm.) is not strictly given, this method nonetheless allows to obtain semiquantitative P-T constraints in rocks, where suitable mineral assemblages are absent. Considering the assemblage muscovitess + chloritess + quartz + H_2O, four reactions can be calculated:

Sample	IQP-P4	IQP-P4	IQP-P4	IQP-P17	IQP-P17	IQP-P17
	ms10	ms11	ms12	ms7	ms8	ms9
SiO_2	46.45	48.42	48.57	47.58	47.76	47.71
TiO_2	0.28	0.39	0.36	0.38	0.24	0.19
Al_2O_3	31.66	30.03	30.40	33.20	33.03	33.30
Cr_2O_3	0.04	0.09	0.05	0.02	n.d.	0.01
Fe_2O_3	2.67	n.c.	n.c.	n.c.	n.c.	n.c.
FeO	1.03	2.76	2.66	2.40	2.44	2.47
MnO	0.04	n.d.	0.01	0.01	n.d.	0.01
MgO	2.07	2.15	2.06	1.33	1.31	1.25
CaO	n.d.	n.d.	n.d.	n.d.	n.d.	n.d.
Na_2O	0.93	0.66	0.50	0.78	0.65	0.80
K_2O	9.39	10.10	10.60	9.99	10.19	10.11
Total	94.57	94.61	95.22	95.70	95.63	95.86
Si	3.130	3.263	3.257	3.161	3.176	3.166
Ti	0.014	0.020	0.018	0.019	0.012	0.009
Al^{IV}	0.870	0.737	0.743	0.839	0.824	0.834
Al^{VI}	1.645	1.649	1.660	1.761	1.765	1.771
Cr	0.002	0.005	0.003	0.001	n.d.	0.001
Fe^{3+}	0.135	n.c.	n.c.	n.c.	n.c.	n.c.
Fe^{2+}	0.058	0.156	0.149	0.133	0.136	0.137
Mn	0.002	n.d.	0.001	0.001	n.d.	0.001
Mg	0.208	0.216	0.206	0.132	0.130	0.124
Ca	n.d.	n.d.	n.d.	n.d.	n.d.	n.d.
Na	0.122	0.086	0.065	0.100	0.084	0.103
K	0.808	0.869	0.908	0.847	0.865	0.857
Sum	6.994	7.000	7.009	6.994	6.992	7.002

Calculations on the base of 11 oxygens, n.d.: not detected; n.c.:not calculated

Table 2

Representative muscovite analyses

Sample	IQP-P2	IQP-P2	IQP-P4	IQP-P4	IQP-P4	IQP-P17	IQP-P17	IQP-P17
	chl1	chl2	chl4	chl5	chl6	chl3	chl4	chl5
SiO_2	25.35	25.15	25.60	25.23	25.01	24.11	24.32	24.07
TiO_2	0.04	0.06	n.d.	0.07	n.d.	0.06	0.08	0.05
Al_2O_3	21.54	20.97	21.75	22.18	22.10	22.32	21.70	23.49
Cr_2O_3	n.d.	n.d.	0.02	0.03	n.d.	0.01	0.06	0.02
Fe_2O_3	n.c.	n.c.	n.c.	n.c.	n.c.	n.c.	n.c.	n.c.
FeO	29.34	29.93	25.57	25.73	25.54	29.68	30.24	30.41
MnO	0.21	0.21	0.15	0.15	0.16	0.24	0.26	0.21
MgO	11.46	11.93	14.82	14.49	14.78	10.86	11.01	10.77
CaO	0.02	0.02	n.d.	n.d.	n.d.	n.d.	n.d.	n.d.
Na_2O	0.09	0.02	0.02	0.02	n.d.	0.03	0.02	n.d.
K_2O	0.02	0.01	0.07	0.05	0.03	0.03	0.03	0.03
Totals	88.07	88.3	88.00	87.95	87.62	87.34	87.72	89.05
Si	2.714	2.698	2.688	2.653	2.640	2.616	2.636	2.563
Ti	0.003	0.005	n.d.	0.006	n.d.	0.005	0.007	0.004
Al^{IV}	1.286	1.302	1.312	1.347	1.360	1.384	1.364	1.437
Al^{VI}	1.433	1.350	1.380	1.403	1.390	1.471	1.409	1.512
Cr	n.d.	n.d.	0.002	0.002	n.d.	0.001	0.005	0.002
Fe^{3+}	n.c.	n.c.	n.c.	n.c.	n.c.	n.c.	n.c.	n.c.
Fe^{2+}	2.627	2.685	2.245	2.263	2.254	2.693	2.741	2.709
Mn	0.019	0.019	0.013	0.013	0.014	0.022	0.024	0.019
Mg	1.828	1.907	2.319	2.271	2.325	1.756	1.779	1.709
Ca	0.002	0.002	n.d.	n.d.	n.d.	n.d.	n.d.	n.d.
Na	0.019	0.004	0.004	0.004	n.d.	0.006	0.004	n.d.
K	0.003	0.001	0.009	0.007	0.004	0.004	0.004	0.004
Sum	9.934	9.974	9.972	9.970	9.987	9.957	9.973	9.959

Calculations on the base of 14 oxygens, n.d.: not detected; n.c.:not calculated

Table 3

Representative chlorite analyses

Sample	IQP-P4	IQP-P4	IQP-P4	IQP-P4
	fsp3 c	fsp9 c	fsp4 r	fsp5 r
SiO_2	65.92	66.35	68.66	68.78
TiO_2	0.01	n.d.	n.d.	n.d.
Al_2O_3	20.26	20.31	18.84	18.91
Cr_2O_3	0.01	n.d.	n.d.	0.01
Fe_2O_3	0.60	0.28	0.24	0.21
FeO	n.c.	n.c.	n.c.	n.c.
MnO	n.d.	0.01	n.d.	0.01
MgO	0.21	n.d.	0.01	n.d.
CaO	1.72	1.87	0.16	0.19
Na_2O	10.26	10.51	11.28	11.35
K_2O	0.05	0.07	0.05	0.06
Totals	99.04	99.40	99.24	99.52
Si	2.922	2.930	3.017	3.015
Ti	n.d.	n.d.	n.d.	n.d.
Al	1.059	1.057	0.976	0.977
Cr	n.d.	n.d.	n.d.	n.d.
Fe^{3+}	0.020	0.009	0.008	0.007
Fe^{2+}	n.c.	n.c.	n.c.	n.c.
Mn	n.d.	n.d.	n.d.	n.d.
Mg	0.014	n.d.	0.001	n.d.
Ca	0.082	0.088	0.008	0.009
Na	0.882	0.900	0.961	0.965
K	0.003	0.004	0.003	0.003
Sum	4.981	4.989	4.973	4.977

Calculations on the base of 8 oxygens, n.d.: not detected; n.c.:not calculated; c: core; r: rim

Table 4

Representative feldspar analyses

(1) 4 clinochlore + 6 pyrophyllite = 26 quartz + 5 Mg-amesite + $2H_2O$

(2) 24 celadonite + 6 pyrophyllite = 26 quartz + 4 muscovite + Mg-amesite + $2H_2O$

(3) celadonite + Mg-amesite = clinochlore + muscovite

(4) 5 Mg-amesite + 6 pyrophyllite = 26 quartz + 5 muscovite + clinochlore + $2H_2O$

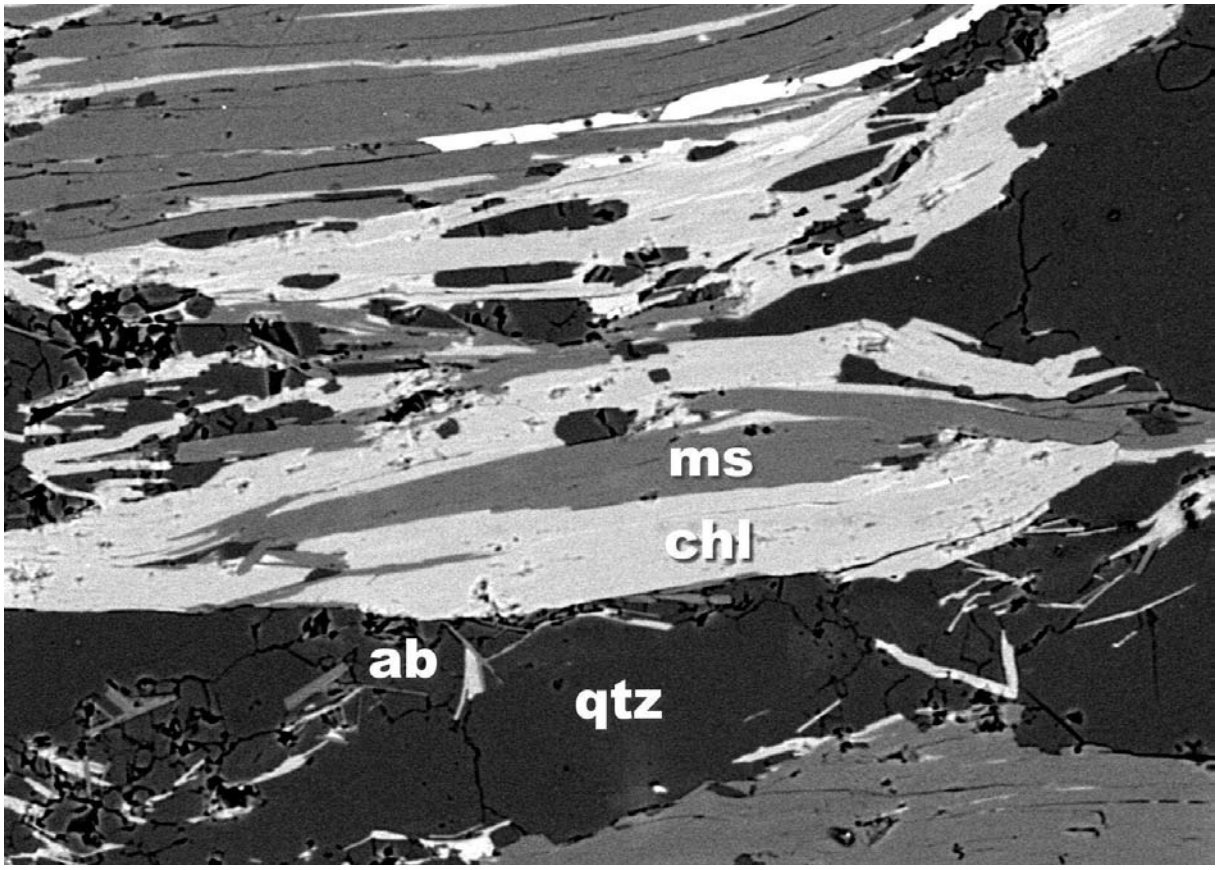

Fig. 3

The BSE image shows the close intergrowth of muscovite and chlorite, which is the requirement for thermobarometric calculations according to the method of VIDAL & PARRA (2000).

The P-T estimates, based upon coexisting muscovite-chlorite pairs, which yield pressures of 4.5 ± 2 kbar at temperatures at 500 ± 50°C, are based upon the intersections between reactions (1) – (4) as shown in Figure 4. Since textural evidence suggests that garnet in this sample is not in equilibrium with the surrounding assemblage muscovite + chlorite + quartz, this method is the only tool to obtain P-T estimates of the samples from the central part of the western IQP.

The method of calculation of all possible equilibria between muscovite + chlorite + quartz was developed by VIDAL & PARRA (2000) and due to the consideration of phase components involving the vacancy on the A-site of muscovite, namely the pyrophyllite component, application of this method is not unproblematic. The subdivision of muscovite and chlorite into its end-members (muscovite, celadonite, pyrophyllite, clinochlore, Mg-amesite) is necessary for calculations and the application of the appropriate activity models of VIDAL & PARRA (2000). Loss of alkali elements during microprobe analysis is therefore a possible source of considerable error. To prevent loss of alkali elements, micas were measured with raster sizes of 3 x 3 μm and 5 x 5 μm. In addition, loss of alkalies was investigated by a series of measurements with varying the counting time, sample current and the raster size.

These investigations only considered the elements Na and K. Sample currents varied from 5 nA to 20 nA. Raster sizes applied were 0.2 μm, 1.5 μm, 2 μm, 3 μm and 6 μm and counting times ranged from 20 to 60 seconds. These measurements showed that variable combinations of all these factors resulted in negligible alkaline loss during peak measurement in the first 20 seconds. Remarkable loss of alkaline elements only occurred after 60 seconds with sample currents of 10 nA and 20 nA.

Since calculation of the hypothetical pyrophyllite component is directly related to the measured value of the vacancy of the A-site, the pyrophyllite activity strongly depends on this value. Calculations of the intersections among the reactions (1) - (4) as shown in Figure 4, yield high uncertainties in P due to small variations in the extent of the A-site vacancy. The calculations have shown that high vacancies on A-site and consequently higher pyrophyllite components yielded higher P. Low contents of the pyrophyllite component yielded shifts to lower P.

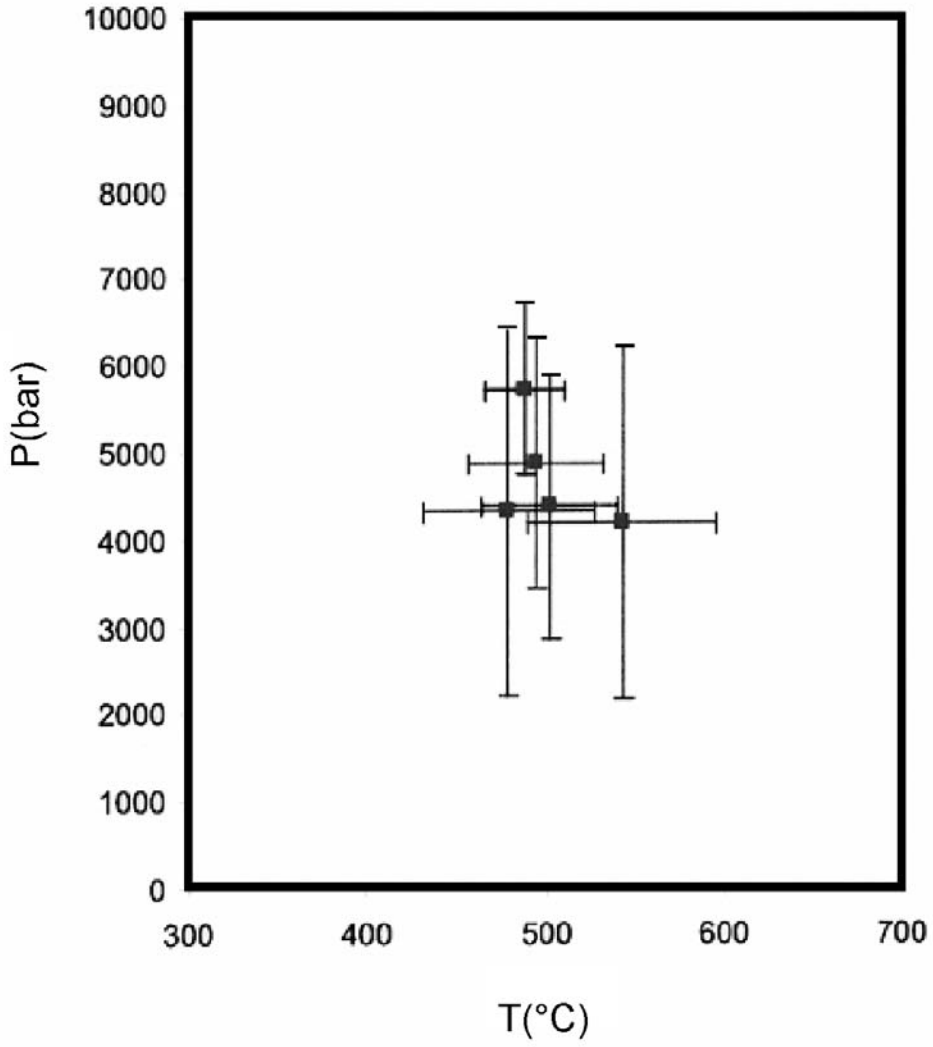

Fig. 4

P-T estimates of sample IQP-P4 of the garnet-micaschist from the central part of the western IQP calculated with the program TWQ v.2.02 using the data set of VIDAL (2002, written comm.) with the assemblage muscovite + chlorite + plagioclase + quartz.

Discussion

Although the western IQP shows petrographical and thermobarometric evidence for a polymetamorphic evolution (PIBER, 2005), geochronological data from the central part of the western IQP indicate a pervasive Permian metamorphic overprint. Zircons, derived from metaporphyroids, which crosscut the western central parts of the IQP yield U/Pb ages which can be interpreted as a T-accentuated Permian event. These ages were also confirmed by Rb/Sr ages of white micas of the IQP (ROCKENSCHAUB et al., 2003). Significant Eo-Alpine re-juvination only occurred in slivers of IQP underneath the Patscherkofel Crystalline Complex (PIBER, 2005). This is in agreement with data from the eastern IQP, where geochronological data also point to a Permian metamorphic event but also a more pervasive Eo-Alpine re-juvination (FÜGENSCHUH, 1995; HANDLER et al., 2000; ANGELMAIER et al., 2000). In contrast to the western IQP, microstructural evidence and the low-T nature of the metamorphic overprint, it is thought that the P-T data of metapelites and the greenschists from the eastern IQP thus correspond to the Eo-Alpine metamorphic overprint (PIBER, 2005; PIBER & TROPPER, 2002, 2007).

Acknowledgments

The authors would like to thank Oliver Vidal for his help with the calculations. Richard Tessadri is thanked for the editorial handling.

References

AMPFERER, O. & OHNESORGE, TH. (1918): Geologische Spezialkarte der Österr.-Ungar. Monarchie, 1:75 000, Blatt Rattenberg (5048). – Wien, Geol. Reichsanstalt.

AMPFERER, O. & OHNESORGE, TH. (1924): Erläuterungen zur geolgischen Spezialkarte der Republik Österreich, 1:75 000, Blatt Innsbruck-Achensee (5047). – Geol. BA, Wien.

ANGELMAIER, P., FRISCH, W. & DUNKL., I. (2000): Thermochronological constraints for the TRANSALP section of the Tauern Window. – 2nd international TRANSALP-Colloquium, Munich, 17.

BERMAN, R. G. (1988): Internally-consistent thermodynamic data for minerals in the system SiO_2-K_2O-Na_2O-Fe_2O_3-TiO_2-Al_2O_3-FeO-MgO-K_2O-H_2O-CO_2. – J. Petrol. 29, 445-522.

BJERG, S. C., MOGESSIE, A. & BJERG, E. (1992): Hyper Form-A hypercard program for the Mac Intosh Microcomputers to calculate mineral formulae from electron microprobe and wet chemical analyses. – Computer & Geoscience 18, 717-745.

FÜGENSCHUH, B. (1995): Thermal and kinematic history of the Brenner area (Eastern Alps, Tyrol). – Unpubl. Ph.D. Thesis, ETH Zürich, 155 p.

GWINNER, M. P. (1971): Geolgie der Alpen. – Stuttgart, Schweizerbart'sche Verlags Buchhandlung, 477 pp.

HADITSCH, G. & MOSTLER, H. (1982): Zeitliche und stoffliche Gliederung der Erzvor-kommen im Innsbrucker Quarzphyllit. – Geol. Paläont. Mitt. Innsbruck, 12, 1-40.

HADITSCH, G. & MOSTLER, H. (1983): The succession of ore mineralization of the lower Austroalpine Innsbruck quartz phyllite. – In: Schneider, H. J. (ed): Mineral deposits in the Alps, Springer Verlag, Berlin-Heidelberg-New York, p. 1-40.

HANDLER, R., GENSER, J., FRIEDL, G., HEIDORN, R., NEUBAUER, F., FRITZ, H. & TENCZER, V. (2000): ^{40}Ar-^{39}Ar ages of white mica from Austroalpine basement units along the TRANSALP section: Tectonic implications. – 2nd international TRANSALP Colloquium, Munich, 17.

HEY, M. J. (1954): A new review of the chlorites. – Min. Mag. 30, 277-292.

HOSCHEK, G., KIRCHNER, E. C., MOSTLER, H., & SCHRAMM, J. M. (1980): Metamorphism in the Austroalpine units between Innsbruck and Salzburg (Austria): a synopsis. – Mitt. Öster. Geol. Ges., 71/72, 335-341.

KOLENPRAT, B., ROCKENSCHAUB, M. & FRANK, W. (1999): The tectonometamorphic evolution of Austroalpine units in the Brenner Area (Tirol, Austria)-structural and tectonic implications. – Tübinger Geowiss. Arb., Ser. A, 52, 116-117.

MOSTLER, H., HEISSEL, G. & GASSER, G. (1982): Untersuchung von Erzlagerstätten im Innsbrucker Quarzphyllit und auf der Alpeiner Scharte. – Arch. f. Lagerst.forsch. Geol. B.-A. Wien, 1, p. 77-83.

PIBER, A. (2005): The metamorphic evolution of the Austroalpine nappes north of the Tauern Window (Innsbruck Quartzphyllite Complex, Patscherkofel Crystalline Complex, Kellerjochgneis and Wildschönau Schist). – Unpubl. PhD Thesis, University of Innsbruck, 261 pp.

PIBER, A. & TROPPER, P. (2002): Multi-equilibrium thermobarometry in low grade metamorphic rocks from the Austroalpine nappes north of the Tauern Window (Kellerjochgneiss, Innsbruck Quartzphyllite). – Mem. Sci. Geol. Vol. 54, 227-231.

PIBER, A. & TROPPER, P. (2007): Metamorphic history of the low grade metamorphic rocks from the crystalline basement nappes north of the Tauern Window (Innsbruck Quartzphyllite, Kellerjochgneiss). – To be submitted to Mineralogy and Petrology.

ROCKENSCHAUB, M., KOLENPRAT, B. & NOWOTNY, A. (2003): Innsbrucker Quarzphyllitkomplex, Tarntaler Mesozoikum, Patscherkofelkristallin. – Arbeitsber. zur Arbeitstagung der Geol. B.-A. in Trins im Gschnitztal 2003, 41-58.

ROTH, R. (1983): Petrographie und Tektonik der mittelostalpinen Kellerjochgneis-Decke und angrenzender Gebiete zwischen Schwaz und Märzengrund (Tirol.) – Unpubl. PhD Thesis, University of Münster, 196 pp.

SATIR, M. & MORTEANI, G. (1978a): Kaledonische, herzynische und alpidische Ereignisse im Mittelostalpin nördlich der westlichen Hohen Tauern, abgeleitet aus petrographischen und geochronologischen Untersuchungen. – Geol. Rundschau, 68, 1-40.

SATIR, M. & MORTEANI, G. (1978b): P-T conditions of the high-pressure Hercynian event in the Alps as deduced from petrological, Rb-Sr and O^{18}/O^{16} data on phengites from the Schwazer Augengneise (EASTERN ALPS, AUSTRIA). – Schweiz. Mineral. Petrograph. Mitt., 58, 289-301.

SATIR, M., FRIEDRICHSEN, H. & MORTEANI, G. (1980): 18O/16O and D/H study of the minerals from the Steinkogelschiefer and the Schwazer Augengneis (Salzburg/Tirol, Austria). – Schweiz. Mineral. Petrograph. Mitt., 60, 99-109.

SCHMIDEGG, O. (1964): Die Ötztaler Schubmasse und ihre Umgebung. – Verh. Geol. Bundesanst., 1957/1, 76-77.

VIDAL, O. & PARRA, T. (2000): Exhumation paths of high pressure metapelites obtained from local equilibria for chlorite-phengite assemblages. – Geol. J., 35, 139-161.

received: 25.06.2007
accepted: 26.06.2007